IEEE Access
Multidisciplinary | Rapid Review | Open Access Journal

IEEE POWER & ENERGY SOCIETY SECTION

Received September 18, 2020, accepted October 4, 2020, date of publication October 7, 2020, date of current version October 19, 2020.

Digital Object Identifier 10.1109/ACCESS.2020.3029273

Integration of Wind and Demand Response for Optimum Generation Reliability, Cost and Carbon Emission

WEI CHIEH KHOO[1], JIASHEN TEH[1], (Member, IEEE), AND CHING-MING LAI[2], (Senior Member, IEEE)

[1]School of Electrical and Electronics Engineering, Universiti Sains Malaysia (USM) at Engineering Campus, Nibong Tebal 14300, Malaysia
[2]Department Electrical Engineering, National Chung Hsing University (NCHU), Taichung 402, Taiwan

Corresponding authors: Jiashen Teh (jiashenteh@usm.my) and Ching-Ming Lai (pecmlai@gmail.com)

This work was supported by the Ministry of Education Malaysia Fundamental Research Grant Scheme (FRGS) under Grant 203/PELECT/6071442.

ABSTRACT Integrating wind power with existing generation systems is one of the most important ways to decarbonise the power sector industry. However, integration must be considered in tandem with its effects towards the adequacy of power supply mainly due to the intermittency of wind. Costs of generators and reliability and carbon emission levels of new wind-integrated generation systems have to be considered. The diversity of demand levels by various load sectors presents an additional pressure on the adequacy of generation system, which should be considered during wind integration. Demand response is effective in relieving the load demands and reducing the number of peaks, but rescheduling energy usage incurs cost to utilities, which should be considered when it is used to aid the integrations of wind power. In this paper, a holistic methodology for optimising the integration of wind power in generation systems is proposed by considering all these factors. Multiple objectives of this optimisation are solved altogether when determining the solution considering their conflicting relationships. Analyses are based on practical data obtained from several real cases. Formulations of the optimisation objectives are generic enough to be useful in other generation systems.

INDEX TERMS Wind, reliability, optimisation, generation system, renewable, demand response, load sectors.

SYMBOL WITHOUT UNIT

k	Auto-regressive constant
w	Moving-average constant
e	Random white noise
μ	Mean value vector of random white noise
Σ	Covariance matrix
V_{ci}	Cut-in wind speed in m/s
V_r	Rated wind speed in m/s
V_{co}	Cut-out wind speed in m/s
$\overline{L(t)}$	DR modified load curve
$L(t)$	Original load curve
Ω	Set of hours when $L(t) > Pk$
Ψ	Set of hours when $L(t) < Pk$
N	Number of hours in Ψ
t	Hour
Lb	Load bus number
Gb	Generation bus number
α	Ratio of generator capacity between 0 and 1 that has been replaced by wind farms
β	Ratio of peak load between 0 and 1, above which the demand is shifted to off-peak hours

SYMBOL WITH UNIT

P_b^W	Wind farm power outputs at bus b in MW
P_r	Rated power capacity of wind farm in MW
Pk	Allowable peak load in MW
P_{Lb}^{loss}	load curtailment of load bus Lb in MWh/y
$VoLL$	Value of load loss in \$/MWh
C	Generator capacity in MW
EPG	Expected power generated in MWh/y
Fix	Fixed costs of generators in (\$/MW)/y
Var	Variable costs of generators in \$/MWh
FOM	Fixed O&M cost in (\$/MW)/y
Cap	Capacity installation cost in (\$/MW)/y
VOM	Variable O&M cost in in \$/MWh

The associate editor coordinating the review of this manuscript and approving it for publication was Ravindra Singh.

Fl	Raw material cost used to generate power in $/MWh
ElecT	Electricity cost of connecting generators to a grid in $/MWh
FlT	Transporting cost of raw material in $/MWh
EDR	Expected demand rescheduled in MWh/y
IC	Load interruption cost in $/MWh
CE	Carbon emission level in tonne/MWh

ABBREVIATION

EECC	Expected energy curtailment cost
EGSC	Expected generation system cost
ELRC	Expected load rescheduling cost
ECEC	Expected carbon emission level
oil	Oil-based combustion turbine and steam generator
cl	coal-based steam generator
ncl	Nuclear steam generators
hy	Hydro plants
wnd	Wind farms
res	Residential load
ind	Industrial load
com	Commercial load
lrg	Large user load
agr	Agriculture load
gov	Governmental load
off	Office load

I. INTRODUCTION

A global consensus holds that a sustainable energy system can be achieved by integrating wind power into power grids due to its main features of no carbon emission and unlimited supply. However, wind farms should achieve grid parity – producing large-scale electricity at prices equal to or cheaper than current practices –for their integrations to be economically viable, and they have been able to do so. However, wind power intermittency is a risk to the reliability of power systems if their integrations become widespread, and limiting wind power to conservative levels is an easy way to mitigate the risk but this limitation unwantedly increases the reliance on fossil fuel [1]. Consequently, various technologies that facilitate the integration of wind without adversely affecting the reliability of power systems are explored.

The battery energy storage system (BESS) has been considered one of the most effective methods owing to its energy storage facility which is crucial for saving excess wind energy for later usage, adjustable size by combining small cell banks together [2], [3] and fast charging response to fill gaps of power and demand mismatch, a feature which conventional large scale generators do not have [4]–[6]. Apart from BESS, pumped-hydro- and flywheel-based mechanisms are effective storage systems but lack deployment flexibility for requiring huge space and have lower energy density compared with a BESS of equal size. As a result, past studies on using energy storage for improving wind integration focused on battery operation modelling [7], [8] and its optimum sizing [9]–[11] and location [12]. In addition to BESS, the dynamic thermal rating (DTR) system is often used on lines connecting wind farms and power networks to enhance the lines' power delivery capacity such that more wind power can be injected into the network, resulting in less wind curtailment [13]. Past studies proved that strategic placement [14], risk-constrained design [15] and line ageing consideration [16], [17] of the DTR system can improve the penetration of wind energy and the reliability of power systems [18]. The reliability modelling of the communication network connecting all DTR sensors that are distributed across large areas [19] has enabled the risk-informed management of lines connected to wind farms [20], which critically prolongs the lines' life, subsequently ensuring the continual absorption of wind power and leading to overall lesser wind curtailment. Despite the advantages of the BESS and the DTR system, the former is limited by its energy density, charging rate, power ratings, roundtrip efficiency and network topology, whereas the latter cannot store energy. Therefore, studies have investigated the combined benefits of the BESS, the DTR system [21] and the DTR system with flexible AC transmission system devices [22] to facilitate the integration of wind energy by compensating one another's drawbacks.

Apart from the BESS and the DTR system, the demand response (DR) programme [23] can mitigate the risk of wind intermittency by levelling the load curve through uniform distributions of load demand across a larger period of time whilst maintaining the same amount of total energy consumption. As a result, the pressure exerted on generators is reduced substantially as peak loads are minimised. The major impetus for DR is the awareness and recognition of the smart meter as one of the major future grid components. Based on smart meters installed at consumers' side and the collected real-time data of electricity usage behaviour, the DR programme allows utilities and consumers to adjust electricity demand for lesser concentration of loads at any time, thereby reducing instances of power supply inadequacy [24]. This result is normally achieved by offering attractive energy pricing schemes through smart meters to incentivise consumers to shift electricity consumption from peak to off-peak times. Therefore, relevant system-wide deployment costs of smart meters are usually justified by customers gaining flexibility in controlling their load demands. In contrast to the BESS and the DTR system, the smart meter is relatively much cheaper and simpler in terms of technological sophistication. Without having to alter network parameters or generation profiles as the DTR system and the BESS do, the DR programme is effective given sufficient participations and cooperation from consumers. Thus, the UK electricity sector has become increasingly open to the DR, which has been previously used in combination with the BESS [25] and the DTR [26] to improve the reliability of wind-integrated generation system without incurring excessive costs, subsequently unlocking greater potential for more integrations of wind power.

None of the previous works addressed the optimisation of wind integration. Previous studies showed that the BESS,

DTR and DR can improve the integration of wind, but the optimum amount of integration was never explored, and no model can determine the optimum wind integration level. More importantly, complex relationships amongst different types of generators that consist of numerous factors such as fixed (capital and maintenance) and variable (fuel, electricity, fuel transportation, ongoing capital and maintenance) costs, effect of system reliability costs and environmental effects due to various carbon emission levels were never considered in all previous studies when dealing with the integration of wind energy. These three factors form the first three drawbacks that this paper intends to address. The act of balancing generator and reliability costs is the universal goal of adequacy and economic assessments of power systems [27], and carbon emission level provides informed decision towards power grid decarbonisations [28]. They are therefore important to be considered in this paper.

Literature reviews also show that the DR programme is more cost effective and easier to implement than the BESS and the DTR in improving wind integration. However, the intricate balance between various levels of DR implementations and cost against various percentages of wind penetration has never been explored. Under the DR program, consumers are normally incentivized to change their load usage pattern, which has to be paid for by utilities [29]. Such a cost has to be considered for a realistic DR program and it represents the load interruption cost in this paper. Load models used in all previous cited DR studies lumped all types of load together without any discrimination between different load sectors such as agriculture, industrial, residential, large users, offices, governmental buildings and commercial, and this approach ignores different incentives normally accorded to different load sectors, leading to less practical DR models which give equal rescheduling emphasis on all load sectors. Therefore, this drawback – the fourth drawback – is addressed in this paper for realistic DR implementations.

The identified research gaps above are summarized:

- Previous studies lack the framework that considers realistic and complex factors such as fixed and variable cost of generators, system reliability costs, carbon emission levels, and different load profiles of various load sectors, when determining the optimum level of wind power and demand response.
- Specific percentages of wind and DR penetrations on all generators and load sectors are never analysed. As a result, optimum levels of wind penetration and DR are not available to utilities.
- Load sectors are never discriminated and lumped altogether, resulting in the failure to identify critical load sectors on which the DR can focus on to reduce load rescheduling cost.

The contributions of this paper are:

- A framework that is able to determine the optimum integration of wind power and implementation of DR together, by minimizing generator costs, reliability cost, carbon emission levels, and DR cost (discrimination amongst load sectors considered), is proposed. The proposed optimization explores the complex relationship amongst these factors. The outcomes are beneficial for vertically integrated utilities who own wind turbines, and are interested to integrate wind power into generation systems for the purpose of decarbonisation without adversely affecting power system reliability and incurring operation costs.
- The proposed framework is able to identify specific wind penetration and DR percentage on each type of generators and load sectors, respectively. A range of optimum results, in the form of Pareto solutions, are obtained to give flexibility to utilities to select the most appropriate solution.
- The discriminations of load sectors carried out in this paper help identify critical load sectors on which the DR program should focus to reduce load rescheduling cost.

II. METHODOLOGY

This section describes the proposed optimization framework for integrating wind and DR. Fig. 1 illustrates the overview.

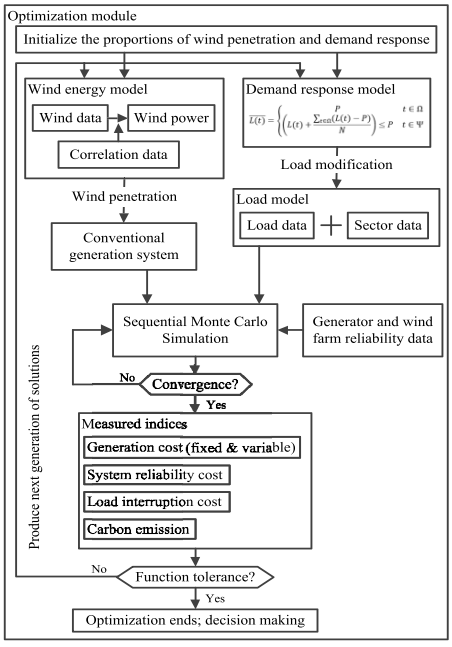

FIGURE 1. Overview of the proposed framework for optimising wind and DR integration.

The proposed framework begins by initialising the optimum proportions of wind penetration and demand response. Wind data of potential wind farm sites are analysed and modelled using the auto-regressive moving-average (ARMA) model, and potential wind power levels are identified (see *wind energy model* in Section II.A), which also considers the correlation of wind data, to determine the amount of wind power available for penetration. Then, data of various load sectors are integrated into the load model (see *Load Model* in Section II. B) to determine the effects of different load interruptions whilst considering the opportunity for

implementing the DR programme (see *Demand Response Model* in Section II.C). Effects of the optimised solution are evaluated in a typical sequential Monte Carlo (SMC) simulation until convergence considering chronological statuses of generators, wind farms and load levels. Indices measured in the SMC simulation are generation fixed and variable costs, system reliability cost, load rescheduling cost due to the DR programme and carbon emission level; their details are available in the *Optimisation Model* in Section II.D. The next set of solutions evolves from current solutions based on common rules of genetic algorithm (GA), and the entire process restarts. Optimisation stops when function tolerance drops below a certain threshold.

A. WIND ENERGY MODEL

One set of historical wind speed data is sampled for each generation bus of the investigated power system, all of which are obtained from the British Atmospheric Data Center (BADC) in an hourly manner from 2006 to 2016 [30]. Historical wind speed data are fitted into the ARMA model to enable the simulation of wind speed and subsequently wind power, which is one of the required inputs of the SMC simulation performed in the proposed optimisation model [31]. The ARMA model is necessary because it can randomly simulate an unlimited number of wind speed values that satisfy the input requirements of SMC simulation. In other words, the number of wind scenarios simulated by the ARMA model matches the simulation number required by the SMC to converge (see section II.E for SMC convergence criteria).

The ARMA model equation consists of two parts, an n-order auto-regressive and an m-order moving average (n, m):

$$y_t = k_1 y_{t-1} + \ldots + k_i y_{t-i} + \ldots + k_n y_{t-n} + e_t - w_1 e_{t-1} - \ldots - w_j e_{t-j} - \ldots - w_m e_{t-m}, \quad (1)$$

where $k_i\,(i = 1, 2, \ldots, n)$ and $w_j\,(j = 1, 2, \ldots, m)$ are the auto-regressive and moving-average constants, respectively; e_t is the random white noise, which is also normally and independently distributed with zero mean and σ^2 variance, notated as $e_t \in NID\left(0, \sigma^2\right)$. The ARMA equation shows that the value of y_t in a future time t is a mean value conditional upon its past observed values, $y_{t-i}\,(i = 1, 2, \ldots, n)$, and random white noise, $e_{t-j}\,(j = 1, 2, \ldots, m)$. In this paper, y_t represents wind speeds.

Correlations of historical wind speed data are considered during simulations of ARMA models; thus, simulated wind speed values retain the same correlation feature. Pearson's product–moment correlation is performed on all historical wind speed data to enable this consideration, as follows:

$$\rho_{x,y} = cov(x, y)\big/\sigma_x \sigma_y, \quad (2)$$

where cov is the covariance between any two historical wind speed vectors notated as x and y, and σ is the standard deviation between the two vectors. Random white noise in (1) of each ARMA model is sampled by considering the correlations calculated in (2) instead of independently of each other and combining normal distribution properties of random white noise of all ARMA models into the equivalent multivariate format as follows:

$$f(x) = \frac{1}{(2\pi)^{\frac{p}{2}} |\Sigma|^{\frac{1}{2}}} \exp\left\{-\frac{1}{2}(x-\mu)^{\mathrm{T}} \Sigma^{-1} (x-\mu)\right\}, \quad (3)$$

where p is the number of ARMA models; μ is the mean value vector of the random white noise of all ARMA models, which is also a zero vector due to zero mean distribution; Σ is the covariance matrix of all ARMA models. Therefore, simulated wind speed is also correlated in the same manner because the covariance matrix guides the simulations of white noise and contains the correlation of historical wind speed data.

Wind farm power outputs at bus b, P_b^W, are determined by considering that the fluctuations of wind speed are negligible within it, as follows [32]:

$$P_b^W = \begin{cases} 0 & 0 \le V_w < V_{ci} \\ \left(A + BV_w + CV_w^2\right) P_r & V_{ci} \le V_w < V_r \\ P_r & V_r \le V_w < V_{co} \\ 0 & V_w \ge V_{co}, \end{cases} \quad (4)$$

where P_r is the rated capacity of the wind farm; V_{ci}, V_r and V_{co} are cut-in, rated and cut-out wind speed of the wind turbine, respectively; constants A, B and C are calculated as follows [21]:

$$A = \frac{1}{(V_{ci}-V_r)^2}\left[V_{ci}(V_{ci}+V_r) - 4(V_{ci}V_r)\left(\frac{V_{ci}+V_r}{2V_r}\right)^3\right],$$
$$B = \frac{1}{(V_{ci}-V_r)^2}\left[4(V_{ci}+V_r)\left(\frac{V_{ci}+V_r}{2V_r}\right)^3 - (3V_{ci}+V_r)\right],$$
$$C = \frac{1}{(V_{ci}-V_r)^2}\left[2 - 4\left(\frac{V_{ci}+V_r}{2V_r}\right)^3\right]. \quad (5)$$

B. LOAD MODEL

Common system load demand data used in most power system reliability analyses ignore the distinctions between load sectors and are all lumped as a single entity [1]. As a result, a load model that recognises individual load sector enables the implementations of the DR programme to be sector specific instead of blanket applications on all sectors. Consequently, this model causes less demand shift and minimally disrupts existing load schedules, leading to less interruption cost due to load rescheduling.

Hence, this paper uses a more comprehensive version of the common load model by recognising that the entire system load demand is composed of various load sectors with a unique pattern for each sector by referring to the aggregate of load demand survey done in [33]. Load sectors identified and considered in the load model of this paper are residential, industrial, commercial, large user, agriculture, governmental and office. Their average composition and demand pattern as

a percentage of the system load in every 24 hours are shown in Fig. 2.

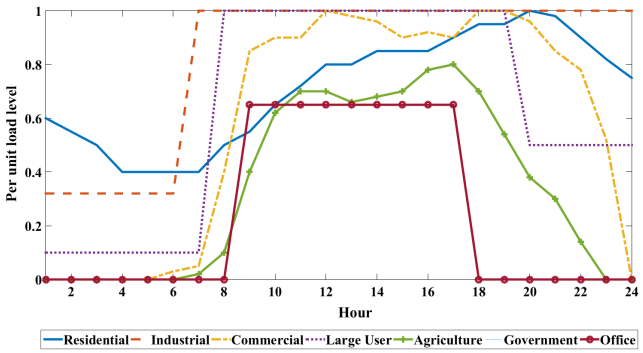

FIGURE 2. Demand patterns of various load sectors considered in this paper.

The figure shows that the demand of each sector generally picks up and is sustained at the highest level during common business hours between around 6 a.m. and 8 p.m. The residential sector is relatively consistent and maintains approximately the same level throughout the day compared with other sectors. Other combinations of load sector pattern may also be used depending on the gathered electricity consumption data, and they will only affect the numerical values of the simulation.

C. DEMAND RESPONSE MODEL

The considered DR programme of this paper shifts the load demand above a certain percentage of the peak load and distributes them equally to off-peak hours when the load level is lower than the percentage threshold, as follows:

$$\overline{L(t)} = \begin{cases} Pk & t \in \Omega \\ \left(L(t) + \dfrac{\sum_{t\in\Omega}(L(t) - Pk)}{N}\right) \leq Pk & t \in \Psi, \end{cases} \tag{6}$$

where $\overline{L(t)}$ and $L(t)$ are the modified and original load demand curves, respectively; Pk is the allowable percentage of peak load; Ω is the set of hours when the original load level is above Pk, also known as on-peak hours; Ψ is the set of hours when the load level is below Pk, also known as off-peak hours; N is the number of hours in Ψ. The second line of (6) shows that the load restoration is also performed by limiting the restored load level to Pk to avoid the formation of new peaks. In instances when new peaks are formed, the remaining load above the peak limit is added to the subsequent hours until all the remaining load has been restored. After all off-peak hours have been considered, remaining loads that cannot be restored are deemed part of load curtailment.

Equation (6) is applied independently on each load sector specified in the load model of Section II.B, which means that the load shifting action is adjustable on each load sector and may differ from one another. It is also worth noting that Pk is dependent on outcomes of the optimization executed in the simulation.

D. OPTIMISATION MODEL

The optimization aims to optimize the penetration of wind power and the implementation of the DR programme, by minimizing expected energy curtailment cost (EECC), expected generation system cost (EGSC), expected load rescheduling cost (ELRC) due to the DR programme and expected carbon emission cost (ECEC). However, these indices have conflicting objectives, and most of them are inversely related with one another. For example, EECC can be kept low by avoiding wind penetration to eliminate intermittency in wind power generations, but this approach has the opposite effect of raising EGSC and ECEC because energy produced by wind farms is cheaper and without carbon emissions. Therefore, all these objectives cannot be minimised as a single function and should be solved as a multi-objective optimisation problem instead, as follows:

$$\min \begin{bmatrix} f_1(t) \\ f_2(t) \\ f_3(t) \\ f_4(t) \end{bmatrix} = \min \begin{bmatrix} \text{EECC}_{Lb}(t) \\ \text{EGSC}_{Gb}(t) \\ \text{ELRC}_{Lb}(t) \\ \text{ECEC}_{Gb}(t) \end{bmatrix}, \tag{7}$$

where it shows that optimisation is performed by considering the chronological development of generation and load demand levels over a specified period, i.e. hourly over a year, and t denotes each hour. Subscript Lb indicates that the indices are relevant only for load buses, whereas Gb indicates generation buses. Details of the four objective functions follow.

Objective 1: To minimise the EECC of power systems:

$$\begin{aligned} \min f_1(t) &= \min\left[\text{EECC}_{Lb}(t)\right] \\ &= \min\left[\sum_{Lb=1}^{L} P_{Lb}^{loss} VoLL\right], \end{aligned} \tag{8}$$

where P_{Lb}^{loss} is the load curtailment of load bus Lb in MWh/y after considering the penetration of wind farms and implementation of the DR programme on each load sector; $VoLL$ is the value of load loss in \$/MWh and is not separated based on load sectors because P_{Lb}^{loss} is the average load loss measurement of all load sectors; and L is the number of load buses.

Objective 2: To minimise EGSC of generation systems:

$$\begin{aligned} &\min f_2(t) \\ &= \min\left[\text{EGSC}_{Gb}(t)\right] \\ &= \min \sum_{Gb=1}^{G} \begin{pmatrix} C_{oil}^{Gb}\left(1-\alpha_{oil}^{GB}\right) Fix_{oil} + EPG_{oil}^{Gb} Var_{oil} \\ C_{cl}^{Gb}\left(1-\alpha_{cl}^{GB}\right) Fix_{cl} + EPG_{cl}^{Gb} Var_{cl} \\ C_{ncl}^{Gb}\left(1-\alpha_{ncl}^{GB}\right) Fix_{ncl} + EPG_{ncl}^{Gb} Var_{ncl} \\ C_{hy}^{Gb}\left(1-\alpha_{hy}^{GB}\right) Fix_{hy} + EPG_{hy}^{Gb} Var_{hy} \\ C_{wnd}^{Gb} Fix_{wd} + EPG_{wnd}^{Gb} Var_{wnd} \end{pmatrix}, \end{aligned} \tag{9}$$

such that

$$C_{wnd}^{Gb} = C_{oil}^{Gb}\alpha_{oil}^{GB} + C_{cl}^{Gb}\alpha_{cl}^{GB} + C_{ncl}^{Gb}\alpha_{ncl}^{GB} + C_{hy}^{Gb}\alpha_{hy}^{GB}, \tag{10}$$

where C is the generator capacity in MW, and EPG denotes the expected power generated in MWh/y; Fix and Var are the fixed and variable costs of generators in ($/MW)/y and $/MWh, respectively; α is the ratio of generator capacity between 0 and 1 that has been replaced by wind farms; all generators are candidates for wind replacement. Subscripts oil, cl, ncl, hy and wnd denote that all variables refer to oil-based combustion turbine and steam generators, coal-based steam generators, nuclear steam generators, hydro plants and wind farms, respectively, at generator bus Gb in a power system with G number of generator buses. Apart from wind farms, all the other generators are specified because they represent the legacy generation system commonly found in existing power systems, such that (9) is generic and applicable in most power systems.

Fixed and variable costs are further defined as follows:

$$Fix_{oil} = FOM_{oil} + Cap_{oil}, \tag{11}$$
$$Fix_{cl} = FOM_{cl} + Cap_{cl}, \tag{12}$$
$$Fix_{ncl} = FOM_{ncl} + Cap_{ncl}, \tag{13}$$
$$Fix_{hy} = FOM_{hy} + Cap_{hy}, \tag{14}$$
$$Fix_{wnd} = FOM_{wnd} + Cap_{wnd}, \tag{15}$$
$$Var_{oil} = VOM_{oil} + Fl_{oil} + ElecT_{oil} + FlT_{oil}, \tag{16}$$
$$Var_{cl} = VOM_{cl} + Fl_{cl} + ElecT_{cl} + FlT_{cl}, \tag{17}$$
$$Var_{ncl} = VOM_{ncl} + Fl_{ncl} + ElecT_{ncl}, \tag{18}$$
$$Var_{hy} = VOM_{hy} + ElecT_{hy}, \tag{19}$$
$$Var_{wnd} = VOM_{wnd} + ElecT_{wnd}, \tag{20}$$

where (11) to (15) describe the consideration of fixed costs, and (16) to (20) describe that for variable costs; FOM and Cap are the one-time cost of fixed operation and maintenance (O&M) and capacity installation in ($/MW)/y, respectively; VOM is the ongoing variable O&M cost throughout the operational period of generators in $/MWh; Fl is the cost of raw materials used to generate power in $/MWh; $ElecT$ is the electricity cost of connecting generators to a grid in $/MWh; FlT is the cost of transporting raw material to generators from material mining sites in $/MWh. (18) shows that although nuclear generators have fuel cost, their fuel transportation cost is negligible because nuclear material is dense and relatively much lighter than other types of materials. Only hydro plants and wind farms have no raw material-related costs because they harvest power from natural sources.

Objective 3: To minimise ELRC of customers:

$$\min f_3(t) = \min\left[\mathrm{ELRC}_{Lb}(t)\right] = \min \sum_{Lb=1}^{L} \begin{pmatrix} EDR_{res}^{Lb}\left(\beta_{res}^{Lb}\right) \times IC_{res} \\ EDR_{ind}^{Lb}(\beta_{ind}^{Lb}) \times IC_{ind} \\ EDR_{com}^{Lb}(\beta_{com}^{Lb}) \times IC_{com} \\ EDR_{lrg}^{Lb}(\beta_{lrg}^{Lb}) \times IC_{lrg} \\ EDR_{agr}^{Lb}(\beta_{agr}^{Lb}) \times IC_{agr} \\ EDR_{gov}^{Lb}(\beta_{gov}^{Lb}) \times IC_{gov} \\ EDR_{off}^{Lb}(\beta_{off}^{Lb}) \times IC_{off} \end{pmatrix}, \tag{21}$$

where EDR is the expected demand rescheduled of a load sector in MWh/y; β is the proportion of peak load ranging between 0 and 1, above which the demand is shifted to off-peak hours based on the DR model in section II.B; IC is the compensation cost for interrupting normal usage patterns due to the DR programme in $/MWh. Subscripts res, ind, com, lrg, agr, gov and off denote that all variables refer to residential, industrial, commercial, large user, agriculture, governmental and office sectors, respectively, at load bus Lb in a power system with L number of load buses.

Objective 4: To minimise ECEC of generation systems:

$$\min f_4(t) = \min\left[\mathrm{ECEC}_{Gb}(t)\right] = \min \sum_{Gb=1}^{G} \left(\begin{pmatrix} EPG_{oil}^{Gb}\left(CE_{oil}^{ct} + CE_{oil}^{st}\right) \\ EPG_{cl}^{Gb} CE_{cl} \end{pmatrix} \times EC \right), \tag{22}$$

where CE denotes the carbon emission level for every MWh of energy produced by fossil fuel generators in tonne/MWh, EC is the emission cost for every tonne of CO_2 emission, and (22) shows that only oil- and coal-based generators emit carbon. Oil-based generators are usually operated with combustion or steam turbine and have different rates of carbon emissions, which are identified in (22) by notations ct and st, respectively. The remaining generators considered in this paper – nuclear, hydro and wind – do not emit carbon.

Optimisations of all the objectives above are performed under the following constraints:

$$\sum_{g=1}^{G} PG_g = \sum_{Lb=1}^{L} PD_{Lb}, \tag{23}$$
$$PG_g^{min} \le PG_g \le PG_g^{max} \tag{24}$$
$$0 \le P_{Lb}^{loss} \le PD_{Lb} \tag{25}$$

where in (23), PG_g is the power generated by each generator g and PD_{Lb} is the power demand of each load bus Lb. In (24), PG_g^{max} and PG_g^{min} are the maximum and minimum power generated by each generator g, respectively. In (25), the maximum load curtailment, P_{Lb}^{loss}, of each load bus Lb is limited to PD_{Lb}.

The proposed optimisation model is executed based on the well-known multi-objective genetic algorithm (MOGA) [34], which is required due to the four conflicting objectives. Moreover, MOGA is suitable because it can handle sophisticated optimisation problems that consider various parameters such as in this paper without imposing any bias on the relationships of the objectives, thus allowing all potential conflicting, supporting or unrelated relationships to be screened. Initialisation of the optimization solutions, α and β, is random based on their constraints, and subsequent optimisations of the solutions are based on common GA procedures such as mutation, combination and crossover [35]. Outcomes of MOGA are a range of non-dominated optimal solutions, also known as the Pareto front, which is achieved when no objectives can be improved without degrading the values of other objectives.

Solutions in the Pareto front are also ranked according to their non-dominancy level.

A solution of the Pareto front is selected based on the fuzzy method due to its ability to model human preferences as mathematical equations [36]. It works by ranking all the Pareto solutions according to the criteria of the decision maker about the objectives in the form of a membership function, as follows:

$$\mu_{f_i}(x) = \begin{cases} 0 & f_i(x) = f_i^{max} \\ \dfrac{f_i^{max} - f_i(x)}{f_i^{max} - f_i^{min}} & f_i^{min} < f_i(x) < f_i^{max} \\ 1 & f_i(x) = f_i^{min}, \end{cases} \quad (26)$$

where $\mu_{f_i}(x)$ is the membership of the i^{th} objective function value, $f_i(x)$, produced by the solution x, which indicates the degree of preference towards x that is obtained from the Pareto front that contains a set of other equally possible solutions, Ω_x; f_i^{min} and f_i^{max} are the minimum and maximum points of the i^{th} objective function, respectively; (23) shows that 1 and 0 membership function values denote complete incompatibility and compatibility, respectively, due to the minimisation problems addressed in the proposed optimisation framework.

Solution x which produces the smallest sum of difference between membership of the objective function, $\mu_{f_i}(x)$, and preference, μ_i, is selected, as follows:

$$\min_{x \in \Omega_x} \sum_{i=1}^{k} \left| \mu_i - \mu_{f_i}(x) \right|^n, \quad (27)$$

where $k = 4$ is the number of objective functions considered in the proposed optimisation model; n is any integer number, and a large number is usually selected to reduce the sensitivity of the final solution towards the setting of preference value, μ_i.

E. SIMULATION PROCEDURE

The simulation of the proposed optimisation framework is described in this section, and the steps are as follows:

Step 1: Determine the ARMA wind speed models of all generation buses where wind farms could be located to replace conventional generators. Hourly wind speeds based on these ARMA models are generated beforehand and will be used later to determine wind power according to the wind energy model in Section II.A if existing generators are replaced with wind farms.

Step 2: Execute the proposed optimisation model, and estimate solutions α^{Gb} and β^{Lb} for all generators and load sectors.

Step 3: Perform SMC simulation to evaluate the effects of the solution on the four objective functions – EECC, EGSC, ELRC and ECEC – considering the random statuses of generators, wind farms and chronological propagation of load sectors for a year. Reliability data of generators are generally available in the investigated power systems. Load models from the power systems are also modified according to the load model and the DR model presented in Section II.B and II.C, respectively. SMC is performed yearly until convergence, i.e. when the variation coefficient of expected energy not supplied is less than 5% or when 100,000 simulations have lapsed.

Locations, capacities, designs, access logistics and maintenance schedules of wind turbines must be determined to determine their reliability data; as a result, the reliability of wind turbine is case specific, and no generic wind turbine reliability data that can be used for study purposes are readily available [37]. Thus, a survey [38] on the reliability of the commonly used wind turbines is examined in this paper. The survey covers data obtained in Denmark, Germany and Sweden, which are countries with reliable, long-term operational records of wind turbines installed at various environments. Hence, the average statistical reliability data derived in the survey is adopted in this paper. The wind turbine based on the directly driven permanent magnet synchronous generator technology is found most reliable, and its failure and repair rates are 1.501/year and 123.6/year, respectively; thus, they are used as the reliability data of wind farms modelled in this paper.

Step 4: Generate the next set of α^{Gb} and β^{Lb} solutions based on the rules of GA, and repeat *Step 3*.

Step 5: Repeat *Step 4* until the function tolerance of MOGA process drops below a certain level.

III. RESULTS AND DISCUSSIONS

The IEEE 24-bus reliability test network (RTN) [39], especially the generation and load data, is used in this paper to demonstrate the proposed optimisation framework. The original generation system of RTN has 10 generation buses, and all are candidate locations for hosting wind farms. Historical wind speed data from 10 different locations in the BADC are sampled and modelled according to the wind energy model, which is then used to calculate wind power output, one for each of the potential wind farms. Details of RTN's original generation system data in Table 1 show the bus, fuel, technology and maximum capacity of each generator. Capacity values are the sum of individual smaller generator capacity of the same type, i.e. same fuel and technology. Based on the classifications in Table 1, 13 candidate generators can be replaced with wind farms, and the degree depends on the outcomes of optimisation. Fixed and variable costs of generators stated in Table 1 [40] and wind farms [27] are shown in Table 2 and 3, respectively; their carbon emission rates [28] and cost [41] are shown in Table 4.

Next, the ramping rates of generators in Table 1 are explained. General Electric (GE) company has recently developed better gas turbine and steam turbine generators that have ramping rate of 50 MW/min [42], and we consider this capability for these two types of generators considered in this paper. The considered ramping rate of nuclear plant is 63MW/min [43]. When extrapolating these two values to an hour, as the SMC is investigated on an hourly basis, it is found that the ramping rates of these generators are well above their

TABLE 1. Generation system data of RTN.

Fuel	Technology	Bus	Capacity (MW)
Oil	Combustion turbine	1	40
		2	40
	Steam turbine	7	300
		13	591
		15	60
Coal	Steam turbine	1	152
		2	152
		15	155
		16	155
		23	660
Light water	Nuclear steam	18	400
		21	400
Water	Hydro turbine	22	300

TABLE 2. Fixed cost of generators.

Fuel	Technology	Cost ((k$/MW)/y)	
		FOM	Cap
Oil	Combustion turbine	10.22	409.00
	Steam turbine		
Coal	Steam turbine	24.52	1,154.00
Light water	Nuclear steam	54.84	2,117.00
Water	Hydro turbine	0.92	1,535.00
Wind	Wind turbine	60.00	1,477.00

TABLE 3. Variable cost of generators.

Fuel	Technology	Cost ($/MWh)			
		VOM	Fl	$ElecT$	FlT
Oil	Combustion turbine	4.09	14.80	16.06	1.30
	Steam turbine				
Coal	Steam turbine	3.07	40.00		0.80
Light water	Nuclear steam	0.43	0.40		-
Water	Hydro turbine	0.003	-		-
Wind	Wind turbine	26.67	-		-

TABLE 4. Carbon emission rates and cost of generators.

Fuel	Technology	CE (tonne/MWh)	EC ($/tonne)
Oil	Combustion turbine	0.618	35
	Steam turbine	0.743	
Coal	Steam turbine	0.835	
Light water	Nuclear steam	--	
Water	Hydro turbine		
Wind	Wind turbine		

considered capacity in this paper. Therefore, when looking from the perspective of hourly time window, the ramping rates of these generators are essentially instantaneous. Ramping rates of hydro plants are generally hard to determine due to effects by reservoir size, water inflow and outflow rates. However, it is generally agreed that hydro plants are fast to react and therefore they can be considered to have instantaneous ramping rate [44]. In this paper, we considered that the size of reservoir is sufficient and water flow rates are fast enough to warrant the instantaneous ramping rate of hydro plants.

Load demand data of the original RTN are modified by incorporating the distribution of seven load sector data in Fig. 2, and their interruption costs due to rescheduling by the DR programme are shown in Table 5 [29]. *VoLL* considered in this paper is $7,500/MWh, which is obtained from the UK Royal Academy of Engineering [45] and is an average value determined from winter and summer data. Based on data presented, the proposed optimisation framework is executed, and the results are presented in this section.

TABLE 5. Interruption cost of load data due to rescheduling.

Load type	IC ($/MWh)
Residential	150
Industrial	13,930
Commercial	12,870
Large user	13,930
Agriculture	650
Governmental	3,460
Office	3,460

A. OPTIMIZATION OUTCOMES

From the 13 candidate generators for wind penetration and 7 candidate load sectors for implementing the DR programme, the proposed optimisation framework considers 20 parameters when searching for the optimum ratios of wind penetration, α, and load shifting, β. The Pareto results are shown in Fig. 3–6.

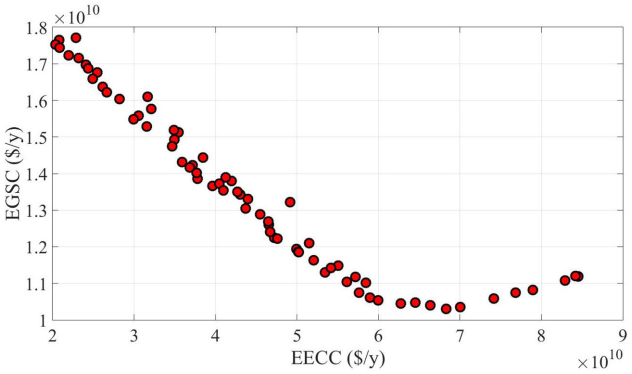

FIGURE 3. EGSC versus EECC.

Fig. 3 shows that EGSC and EECC are inversely related. When EGSC increases, the penetration of wind farms decreases, and more CGUs are used to supply power demand. Most of the EGSC index values are contributed by CGUs because they are more expensive to operate than wind farms. Total power supply fluctuates less due to the lower dependency on intermittent wind power with the reduction of wind farm operations. Under this condition with greater system adequacy and more stable power supply coming from CGUs, more load demand can be matched, and EECC decreases. By extension, ECEC increases as more CGUs operate due

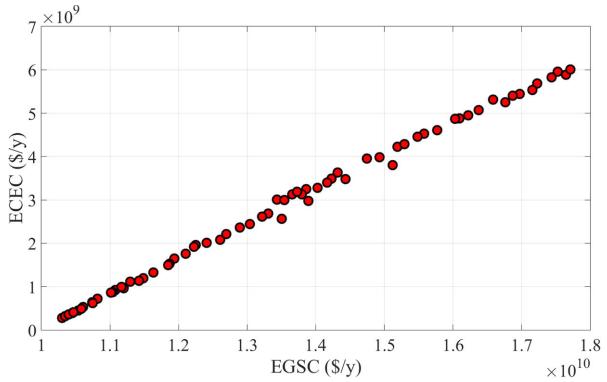

FIGURE 4. ECEC versus EGSC.

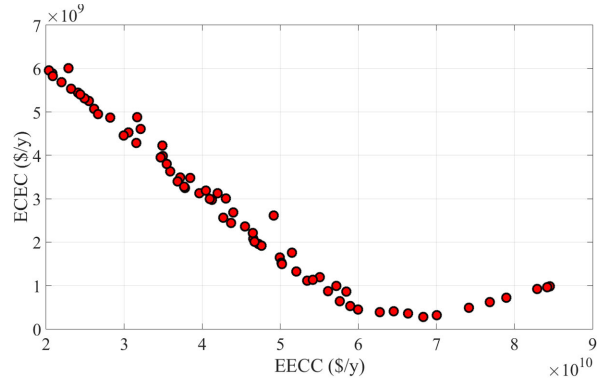

FIGURE 5. ECEC versus EECC.

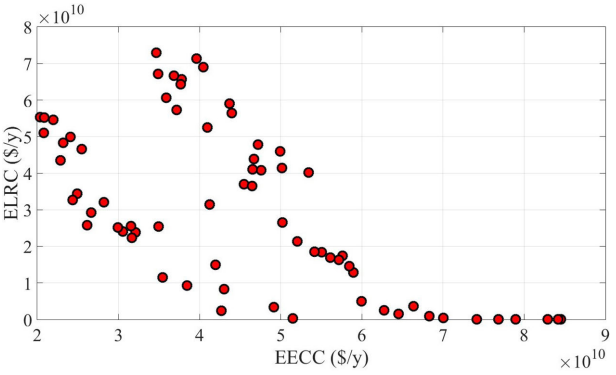

FIGURE 6. ELRC versus EECC.

to more carbon emissions from burning fossil fuels when generating electricity, which forms an almost directly proportional relationship with EGSC, as shown in Fig. 4. As a result, the plot of ECEC against EECC in Fig. 5 is also inversely related in a trend similar to that of Fig. 3. Another reason for the similarity is that to reduce EECC, the optimisation searches for solutions with a higher share of CGUs to provide greater power adequacy, which is more reliable than wind power, and EGSC increases, which is followed by higher ECEC due to more utilisation of fossil fuel. The relationship between ELRC and EECC is studied and plotted in Fig. 6. In general, ELRC and EECC are inversely related, but the trend is not as strong as that of the other figures. The increment in ELRC signifies that a greater percentage of peak demand is shifted, leading to lower peak in the new demand pattern, and vice versa. Therefore, as ELRC increases, flatter load demand patterns are produced. Consequently, EECC decreases as demands are matched more easily by power supply.

Based on the equal priority of all optimisation objectives, i.e. $\mu_1 = \mu_2 = \mu_3 = \mu_4 = 0.5$ and applying the fuzzy decision-making method in (23) and (24), a set of Pareto solutions that consist of wind penetration ratios in all candidate generators, i.e. α, and load shifting ratios in all load sectors, i.e. β, is obtained, as shown in Fig. 7. This set of prioritisation yields 71.56% of wind penetration in the RTN generation system, which is equal to 2,436.56 MW of wind power. Profiles of initial RTN generation system and wind power are illustrated in Fig. 8.

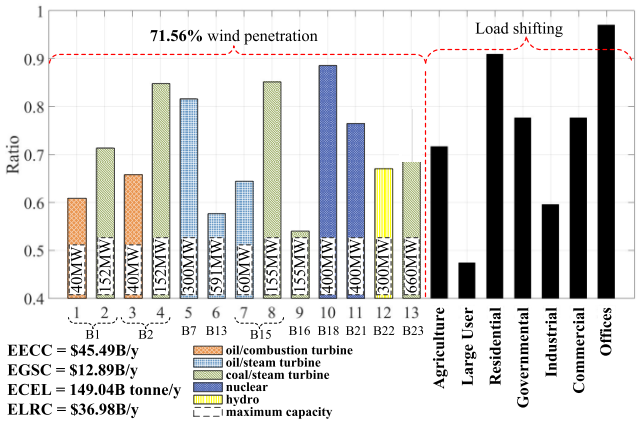

FIGURE 7. Wind penetration and load shifting ratios with equal priority of all optimisation objectives.

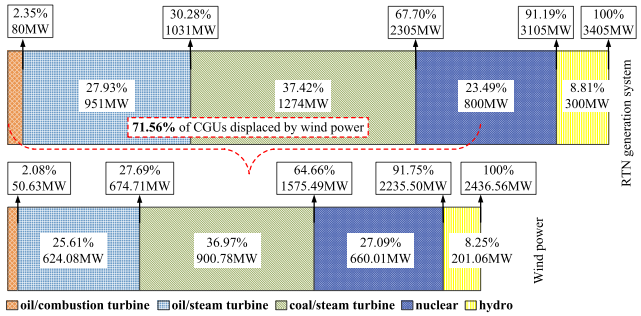

FIGURE 8. Profiles of initial RTN generation system and wind power displacement in each CGU based on equal prioritisation of EECC, EGSC, ECEC and ELRC.

Fig. 8 shows that amongst the five types of CGUs, coal-fired steam turbine generators are displaced by wind power the most by 36.97%. The reason is that this generator group, which constitutes 37.42% of the RTN generation system, is the largest amongst all types of CGUs; it has the second largest carbon emission potential after oil-based generators, which is 752 tonne/hour or approximately 45% of maximum RTN carbon emission level in each hour. Nuclear generators, which constitute 23.49% of the RTN generation capacity, comprise the third largest CGU group but have the second

highest percentage of wind power displacements of as much as 27.09%. The reason is that nuclear generators have the highest fixed cost, which is more than the second highest fixed cost given by a hydro plant by a substantial 42%. Therefore, replacing nuclear generators with wind farms can considerably lower EGSC. Oil-fired steam turbine generators have the third highest percentage of capacity displaced by wind, which is 25.61%. Although the percentage capacity of this generator group is the second highest and 4.44% higher than that of nuclear generators in RTN, optimisation ultimately determines that slightly reducing wind penetration in this generator group in favour of nuclear generators can achieve the balance between EGSC and ECEC due to equal prioritisation in all optimisation objectives when selecting a Pareto solution. However, the combined wind penetration percentage in both types of oil-fired generators irrespective of the generator technology, which is 27.69%, remains higher than nuclear's alone, albeit only slightly by 0.6%. Oil-fired combustion turbine generators have the least capacity displaced by wind power followed by hydro plant, i.e. 2.08% and 8.25%, respectively, because both CGU groups constitute only small portions of the RTN generation capacity, which are 2.35% and 8.81%, respectively.

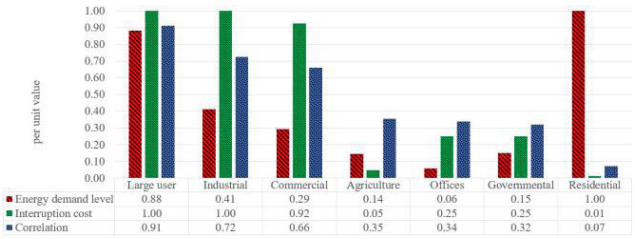

FIGURE 9. Load shifting ratios of all load sectors arranged in the order of decreasing correlation.

Energy demand level and interruption cost of all load sectors are analysed and plotted in Fig. 9 to explain the outcomes of load shifting ratios shown on the right-hand side of Fig. 7 because these two factors influence the ratio values. The values of both factors are expressed on the per unit basis by using their respective largest class as base values. The highest energy demand level comes from the residential sector, which has 5,201 GWh of energy demand throughout the year. The most expansive interruption cost is \$13,930/MWh given equally by industrial and large user sectors. Load sectors with higher interruption cost and energy demand level will undergo more load shifting. However, the plot in Fig. 9 shows that the specific contributions of these factors towards the load shifting ratios cannot be identified. For example, the commercial sector, which is higher than the agriculture sector in energy demand level and load interruption cost, is assigned a higher load shifting ratio, than the agriculture sector i.e. less demand is shifted as the allowable peak load is higher. Moreover, the residential sector with a drastically higher energy demand level than the governmental sector is also assigned a higher load shifting ratio.

Due to this, the correlations between ELRC and load shifting ratio in all Pareto solutions of all load sectors are determined to identify the share of contribution of each sector towards the ELRC index, as shown in Fig. 9. The figure also ranks sectors in decreasing order according to the correlation values, which suggest that ELRC index value is mostly determined by the amount of load shifted in the large user sector, followed by the industrial sector. Load shifting ratio should be the lowest, i.e. most load is shifted, starting from the large user sector and gradually increases in other sectors in the order of arrangement along the x-axis of Fig. 9. However, load shifting ratios in Fig. 7 show that this deduction is only applicable in large user and industrial sectors and not on all the other sectors. This deduction can be explained by plotting load shifting ratios across all Pareto solutions based on the increasing order of ELRC index, as shown in Fig. 10 for large user and industrial sectors, and Fig. 11 for all the other sectors.

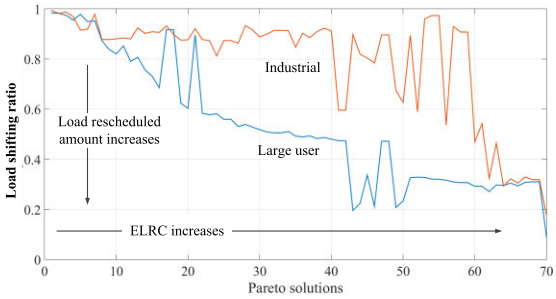

FIGURE 10. Load shifting ratio of large user and industrial sectors as ELRC increases.

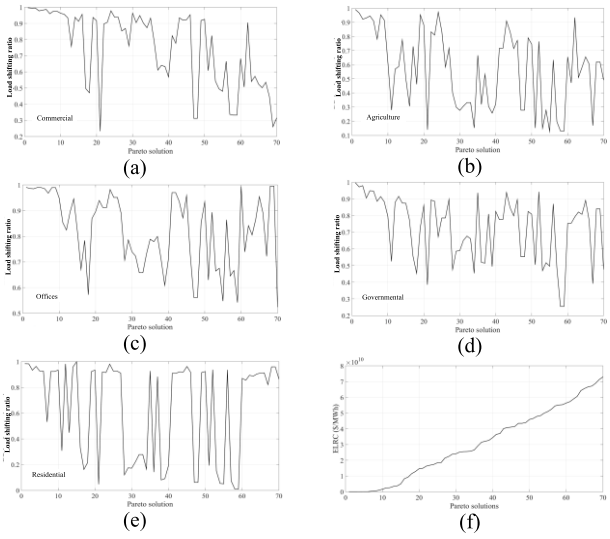

FIGURE 11. Load shifting ratio of (a) commercial, (b) agriculture, (c) offices, (d) governmental and (e) residential sectors as ELRC increases and (f) overall ELRC of all Pareto solutions ranked in ascending order.

Fig. 10 shows a strong trend of reduction in the load shifting ratio of the large user sector, and the trend weakens in the industrial sector as the correlation decreases 20.9% from 0.91 to 0.72; the points of the 40th Pareto solution are the same as Fig. 7. In general, both lines in Fig. 10 decrease as

ELRC increases, but several outliers spike from their trend lines where the load shifting ratio is not consistently decreasing, which is more apparent in the industrial than the large user sector. Outliers exist due to various degrees of hourly fluctuations of load demand in all sectors, which complicate the effects of energy demand levels and interruption costs on load shifting ratios. Fig. 11(a)–(e) show that correlations in all the other sectors are very weak to form trends that track the load shifting ratios. Their ratios are so scattered that their ranking in Fig. 9 does not corroborate the deduction that load shifting ratio increases as correlation decreases. However, collective ratios of all sectors contribute to ELRCs that display a consistently increasing trend when ranked in ascending order, as shown in Fig. 11(f).

Therefore, combined effects of hourly load fluctuations, demand levels and interruption costs contribute to load shifting ratios in a non-linear, fairly unpredictable manner. The large user sector generally owns the lowest load shifting ratio in as much as 44% of Pareto solutions. By contrast, the industrial sector owns the second lowest ratio in only 26% of the time. The remaining positions are randomly owned by other sectors.

Effects of wind penetration percentage on EECC, EGSC and ECEC are analysed and plotted on the y-logarithmic scale, as shown in Fig. 12. The results in this figure are obtained by ranking the Pareto solution based on the percentage of wind penetration in ascending order. The figure also shows the linear equations of trend lines of all indices, which indicate that ECEC is most sensitive towards variation of wind power penetration because it has the highest slope value.

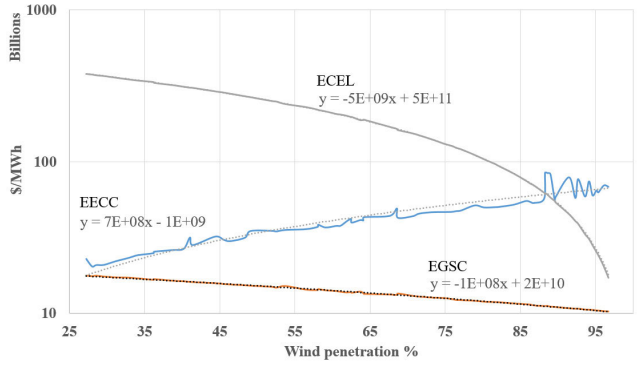

FIGURE 12. Effects of wind penetration percentage on EECC, EGSC and ECEC.

IV. CONCLUSION

In this paper, an optimisation framework for wind power integrations considering EECC, EGSC, ELRC due to the DR programme and ECEC is proposed. EECC index considers overall reliability effects of wind power displacements and interactions between the new generation system and the new load demand pattern due to the implementation of the DR programme, which affects ELRC. Wind farms reduce ECEC drastically, and this benefit is balanced with EGSC to ensure a sustainable generation system from the economic perspective. Parameters such as value of load loss, generation fixed and variable costs, demand variations due to various load sectors and their corresponding interruption costs due to demand rescheduling and carbon emission levels of various fossil fuel generators are considered to make the formulations of all four optimisation objectives robust and practical. Solutions obtained from this proposed framework provide options that a decision maker can select based on various priority levels of optimisation objectives, whose ranking is customisable. On the basis of balanced, equal priority ranking of all objectives, the percentage of wind penetration is 71.56%. The large user load sector also contributes the majority of ELRC in 44% of all Pareto solutions.

For future studies, different ramping rates of generators should be explored and new studies investigating effects of various ramping rates towards the integration of wind is suggested. Next, it is worth pointing out that various rates of energy recovery, the feasibility of them being recovered during off-peak hours, and the further classifications of load sectors into different types of loads, i.e., controllable and non-controllable load, air conditioning load, lighting load and etc., and their consumption behaviours are not considered in the proposed DR model. These factors should be considered also in future studies and be included on top of the proposed optimisation model of this paper. Finally, effects of reservoir and water inflow capacities are considered to be always sufficient to warrant the instantaneous ramping rate of hydro plants modelled in this paper. These factors are worth exploring as future studies in order to examine their effects on the percentage of wind integration and DR deployment.

REFERENCES

[1] H. Abunima, J. Teh, C.-M. Lai, and H. Jabir, "A systematic review of reliability studies on composite power systems: A coherent taxonomy motivations, open challenges, recommendations, and new research directions," *Energies*, vol. 11, no. 9, p. 2417, Sep. 2018.

[2] F. Mohamad and J. Teh, "Impacts of energy storage system on power system reliability: A systematic review," *Energies*, vol. 11, no. 7, p. 1749, Jul. 2018.

[3] F. Mohamad, J. Teh, C.-M. Lai, and L.-R. Chen, "Development of energy storage systems for power network reliability: A review," *Energies*, vol. 11, no. 9, p. 2278, Aug. 2018.

[4] A. Bani Ahmad, C. A. Ooi, D. Ishak, and J. Teh, "State-of-charge balancing control for ON/OFF-line internal cells using hybrid modular multilevel converter and parallel modular dual L-bridge in a grid-scale battery energy storage system," *IEEE Access*, vol. 7, pp. 131–147, 2019.

[5] C.-M. Lai, Y.-H. Li, Y.-H. Cheng, and J. Teh, "A high-gain reflex-based bidirectional DC charger with efficient energy recycling for low-voltage battery charging-discharging power control," *Energies*, vol. 11, no. 3, p. 623, Mar. 2018.

[6] C.-M. Lai, Y.-H. Cheng, J. Teh, and Y.-C. Lin, "A new combined boost converter with improved voltage gain as a battery-powered front-end interface for automotive audio amplifiers," *Energies*, vol. 10, no. 8, p. 1128, Aug. 2017.

[7] Y. Zhang, S. Zhu, and A. A. Chowdhury, "Reliability modeling and control schemes of composite energy storage and wind generation system with adequate transmission upgrades," *IEEE Trans. Sustain. Energy*, vol. 2, no. 4, pp. 520–526, Oct. 2011.

[8] T.-C. Hung, J. Chong, and K.-Y. Chan, "Reducing uncertainty accumulation in wind-integrated electrical grid," *Energy*, vol. 141, pp. 1072–1083, Dec. 2017.

[9] F. Mohamad, J. Teh, and H. Abunima, "Multi-objective optimization of solar/wind penetration in power generation systems," *IEEE Access*, vol. 7, pp. 169094–169106, 2019.

[10] S. Bahramirad, W. Reder, and A. Khodaei, "Reliability-constrained optimal sizing of energy storage system in a microgrid," *IEEE Trans. Smart Grid*, vol. 3, no. 4, pp. 2056–2062, Dec. 2012.
[11] J. Dong, F. Gao, X. Guan, Q. Zhai, and J. Wu, "Storage-reserve sizing with qualified reliability for connected high renewable penetration micro-grid," *IEEE Trans. Sustain. Energy*, vol. 7, no. 2, pp. 732–743, Apr. 2016.
[12] M. Ghofrani, A. Arabali, M. Etezadi-Amoli, and M. S. Fadali, "Energy storage application for performance enhancement of wind integration," *IEEE Trans. Power Syst.*, vol. 28, no. 4, pp. 4803–4811, Nov. 2013.
[13] J. Teh, C.-M. Lai, N. A. Muhamad, C. A. Ooi, Y.-H. Cheng, M. A. A. M. Zainuri, and M. K. Ishak, "Prospects of using the dynamic thermal rating system for reliable electrical networks: A review," *IEEE Access*, vol. 6, pp. 26765–26778, 2018.
[14] J. Teh and I. Cotton, "Critical span identification model for dynamic thermal rating system placement," *IET Gener., Transmiss. Distrib.*, vol. 9, no. 16, pp. 2644–2652, Dec. 2015.
[15] J. Teh and I. Cotton, "Risk informed design modification of dynamic thermal rating system," *IET Gener., Transmiss. Distrib.*, vol. 9, no. 16, pp. 2697–2704, Dec. 2015.
[16] J. Teh, C.-M. Lai, and Y.-H. Cheng, "Impact of the real-time thermal loading on the bulk electric system reliability," *IEEE Trans. Rel.*, vol. 66, no. 4, pp. 1110–1119, Dec. 2017.
[17] J. Teh, "Uncertainty analysis of transmission line end-of-life failure model for bulk electric system reliability studies," *IEEE Trans. Rel.*, vol. 67, no. 3, pp. 1261–1268, Sep. 2018.
[18] J. Teh and I. Cotton, "Reliability impact of dynamic thermal rating system in wind power integrated network," *IEEE Trans. Rel.*, vol. 65, no. 2, pp. 1081–1089, Jun. 2016.
[19] J. Teh and C.-M. Lai, "Reliability impacts of the dynamic thermal rating system on smart grids considering wireless communications," *IEEE Access*, vol. 7, pp. 41625–41635, 2019.
[20] J. Teh and C.-M. Lai, "Risk-based management of transmission lines enhanced with the dynamic thermal rating system," *IEEE Access*, vol. 7, pp. 76562–76572, 2019.
[21] J. Teh and C.-M. Lai, "Reliability impacts of the dynamic thermal rating and battery energy storage systems on wind-integrated power networks," *Sustain. Energy, Grids Netw.*, vol. 20, Dec. 2019, Art. no. 100268.
[22] J. Teh, C.-M. Lai, and Y.-H. Cheng, "Improving the penetration of wind power with dynamic thermal rating system, static VAR compensator and multi-objective genetic algorithm," *Energies*, vol. 11, no. 4, p. 815, Apr. 2018.
[23] H. Jabir, J. Teh, D. Ishak, and H. Abunima, "Impacts of demand-side management on electrical power systems: A review," *Energies*, vol. 11, no. 5, p. 1050, Apr. 2018.
[24] H. J. Jabir, J. Teh, D. Ishak, and H. Abunima, "Impact of demand-side management on the reliability of generation systems," *Energies*, vol. 11, no. 8, p. 2155, Aug. 2018.
[25] J. Teh, "Adequacy assessment of wind integrated generating systems incorporating demand response and battery energy storage system," *Energies*, vol. 11, no. 10, p. 2649, Oct. 2018.
[26] J. Teh, C. Ooi, Y.-H. Cheng, M. A. M. Zainuri, and C.-M. Lai, "Composite reliability evaluation of load demand side management and dynamic thermal rating systems," *Energies*, vol. 11, no. 2, p. 466, Feb. 2018.
[27] *Renewable Power Generation Costs in 2017*, Int. Renew. Energy Agency (IRENA), Abu Dhabi, United Arab Emirates, 2018.
[28] R. Hemmati, H. Saboori, and M. A. Jirdehi, "Multistage generation expansion planning incorporating large scale energy storage systems and environmental pollution," *Renew. Energy*, vol. 97, pp. 636–645, Nov. 2016.
[29] P. J. Balducci, J. M. Roop, L. A. Schienbein, J. G. DeSteese, and M. R. Weimar, "Electrical power interruption cost estimates for individual industries, sectors, and U.S. economy," Pacific Northwest Nat. Lab., Richland, WA, USA, Tech. Rep., 2002.
[30] *British Atmospheric Data Center (BADC)*. Accessed: Oct. 8, 2020. [Online]. Available: http://badc.nerc.ac.uk/home/
[31] P. M. T. Broersen, "Automatic spectral analysis with time series models," *IEEE Trans. Instrum. Meas.*, vol. 51, no. 2, pp. 211–216, Apr. 2002.
[32] P. Giorsetto and K. F. Utsurogi, "Development of a new procedure for reliability modeling of wind turbine generators," *IEEE Trans. Power App. Syst.*, vol. PAS-102, no. 1, pp. 134–143, Jan. 1983.
[33] D. Huang and R. Billinton, "Effects of load sector demand side management applications in generating capacity adequacy assessment," *IEEE Trans. Power Syst.*, vol. 27, no. 1, pp. 335–343, Feb. 2012.
[34] N. Samaan, "Reliability assessment of electric power systems using genetic algorithms," Ph.D. dissertation, Texas A&M Univ., College Station, TX, USA, Aug. 2004.
[35] D. E. Goldberg, *Genetic Algorithm in Search, Optimization, and Machine Learning*. Reading, MA, USA: Addison-Wesley, 1989.
[36] J. Maiers and Y. S. Sherif, "Applications of fuzzy set theory," *IEEE Trans. Syst., Man, Cybern.*, vol. SMC-15, no. 1, pp. 175–189, Jan./Feb. 1985.
[37] F. Spinato, P. J. Tavner, G. J. W. van Bussel, and E. Koutoulakos, "Reliability of wind turbine subassemblies," *IET Renew. Power Generat.*, vol. 3, no. 4, pp. 387–401, Dec. 2009.
[38] Q. Gao, B. Xie, X. Cai, and C. Liu, "Evaluation of the mainstream wind turbine concepts considering their reliabilities," *IET Renew. Power Gener.*, vol. 6, no. 5, pp. 348–357, Sep. 2012.
[39] C. Grigg, P. Wong, P. Albrecht, R. Allan, M. Bhavaraju, R. Billinton, Q. Chen, C. Fong, S. Haddad, S. Kuruganty, W. Li, R. Mukerji, D. Patton, N. Rau, D. Reppen, A. Schneider, M. Shahidehpour, and C. Singh, "The IEEE reliability test system-1996. A report prepared by the reliability test system task force of the application of probability methods subcommittee," *IEEE Trans. Power Syst.*, vol. 14, no. 3, pp. 1010–1020, Aug. 1999.
[40] H. Zerriffi, H. Dowlatabadi, and A. Farrell, "Incorporating stress in electric power systems reliability models," *Energy Policy*, vol. 35, no. 1, pp. 61–75, Jan. 2007.
[41] I. Parry, "Putting a price on pollution," *Finance Develop.*, vol. 56, no. 4, Dec. 2019.
[42] *Innovation Landscape Brief: Flexibility in Conventional Power Plants*, Int. Renew. Energy Agency, Abu Dhabi, United Arab Emirates, 2019.
[43] *Nuclear Energy Factsheets—Load Following Capabilities of Nuclear Power Plants*, SNETP, Brussels, Belgium, 2017.
[44] B. Kirby and M. Miligan, "A method and case study for estimating the ramping capability of a control area or balancing authority and implications for moderate or high wind penetration," Nat. Renew. Energy Lab., Golden, CO, USA, Tech. Rep., 2005.
[45] "Counting the cost: The economic and social costs of electricity shortfalls in the UK," Roy. Acad. Eng., London, U.K., Tech. Rep., Nov. 2014.

WEI CHIEH KHOO received the B.Eng. degree in mechanical engineering from Universiti Tenaga Nasional (UNITEN), Selangor, Malaysia, in 2008, and the M.B.A. degree from Universiti Sains Malaysia (USM), in 2016, where he is currently pursuing the Ph.D. degree in power and energy.

JIASHEN TEH (Member, IEEE) received the B.Eng. degree (Hons.) in electrical and electronics engineering from Universiti Tenaga Nasional (UNITEN), Selangor, Malaysia, in 2010, and the Ph.D. degree in similar field from The University of Manchester, Manchester, U.K., in 2016.

In 2018, he was appointed and served as an Adjunct Professor at the Green Energy Electronic Center, National Taipei University of Technology (Taipei Tech), Taipei, Taiwan. Since 2019, he has been an Adjunct Professor with the Intelligent Electric Vehicle and Green Energy Center, National Chung Hsing University (NCHU), Taichung, Taiwan. Since 2016, he has been a Senior Lecturer/Assistant Professor with Universiti Sains Malaysia (USM), Penang, Malaysia. His research interests include the probabilistic modeling of power systems, the grid-integration of renewable energy sources, and the reliability modeling of smart grid networks.

Dr. Teh is a Chartered Engineer (C.Eng.) conferred by the Engineering Council, U.K., and the Institution of Engineering and Technology (IET), a registered Professional Engineer (P.Eng.) of the Board of Engineers Malaysia (BEM), and a member of the IEEE Power and Energy Society and the Institution of Engineers Malaysia (IEM). He received the outstanding publication awards from the USM in 2017 and 2018. He is also a regular invited Reviewer of the *International Journal of Electrical Power and Energy Systems*, IEEE Access, IEEE Transactions on Industry Applications, IEEE Transactions on Vehicular Technology, IEEE Transactions on Reliability, IEEE Transactions on Industrial electronics, and the *IET Generation, Transmission, and Distribution*.

CHING-MING LAI (Senior Member, IEEE) received the Ph.D. degree in electrical engineering from National Tsing Hua University, Hsinchu, Taiwan, in 2010.

From 2009 to 2012, he served as a Senior Research and Development Engineer with Lite-ON Technology Corporation, Taiwan, where he worked on high-efficiency and high-power-density power supply. In 2012, he established UPE-Power Technology Company, Ltd., Taichung, Taiwan, the company is mainly developing switching power supplies. From 2014 to 2019, he was a Faculty Member of the Department of Vehicle Engineering, National Taipei University of Technology (Taipei Tech). Since 2019, he has been an Associate Professor with the Department of Electrical Engineering, National Chung Hsing University (NCHU), Taiwan, where he is also the Director of the Intelligent Electric Vehicle and Green Energy Center (i-Center). His research interests include electric vehicles (EVs), power electronics, and high-efficiency energy power conditioning systems.

Dr. Lai is an IET Fellow, and a Life Member of the Taiwan Power Electronics Association (TaiPEA), the Society of Automotive Engineers Taipei (SAE-Taipei), the Chinese Institute of Electrical Engineering (CIEE), the Chinese Institute of Engineers (CIE), the Taiwan Association of Systems Science and Engineering (TASSE), and the Taiwan Power and Energy Engineer Association. Besides, he joins as the Society Member of the IEEE Power Electronics, IEEE Industry Applications, IEEE Industrial Electronics, and IEEE Circuits and Systems. He received the Best Paper Award from the IEEE International Conference on Power Electronics and Drive Systems in 2013. He was the recipient of the Young Author's Award for Practical Application from the Society of Instrument and Control Engineers (SICE), Japan, in 2008. He received the Best Paper Award of three papers from the TaiPEA from 2007 to 2010, one Excellent Paper Award from the National Symposium on Taiwan Electrical Power Engineering in 2009, and two Excellent Paper Awards from the Annual Conference of SAE-Taipei in 2016 and 2017. From 2017 to 2018, he was named as an Outstanding Researcher by the College of Mechanical and Electrical Engineering, Taipei Tech. In 2018, he was awarded the Dr. Shechtman Youth Researcher Award by Taipei Tech, the Outstanding Youth Electrical Engineer Award by the Chinese Institute of Electrical Engineering, the Special Outstanding Talent Award by the Ministry of Science and Technology, and the Outstanding Education Achievement Award by the SAE-Taipei. In 2019, he received the Outstanding Youth Control Engineer Award by the Chinese Automatic Control Society. He was named as an Outstanding Youth Engineer Award by the Chinese Institute of Engineers-Taichung Chapter. Since 2017, he has been serving as an Editor of the IEEE TRANSACTIONS ON VEHICULAR TECHNOLOGY.